Can. J. Remote Sensing, Vol. 36, Suppl. 1, pp. S13–S25, 2010

MAGIC: MAp-Guided Ice Classification System

D.A. Clausi, A.K. Qin, M.S. Chowdhury, P. Yu, and P. Maillard

Abstract. A MAp-Guided Ice Classification (MAGIC) system is described and demonstrated. MAGIC is designed specifically to read and interpret synthetic aperture radar (SAR) sea ice images using associated ice maps as provided by the Canadian Ice Service (CIS). An ice chart is manually created at the CIS based on the corresponding SAR image and other ancillary data to provide ice concentrations, types, and floe sizes within enclosed "polygon" regions. MAGIC uses such information as input and then generates a sensor resolution (pixel-based) ice map for each polygon, a product not feasibly produced manually. The primary feature of the current MAGIC version 1.0 is its segmentation module, which is evaluated successfully on a number of images. MAGIC is designed to be used not only as a specific tool for sea ice interpretation but also as a general platform for interpreting generic digital imagery using implemented fundamental and advanced algorithms.

Résumé. On fait la description et la démonstration du système MAGIC (« MAp-Guided Ice Classification »). Le système MAGIC est conçu spécifiquement pour lire et interpréter les images radar à synthèse d'ouverture (RSO) de la glace de mer à l'aide des différentes cartes des glaces telles que celles produites par le Service canadien des glaces (SCG). Une carte des glaces est créée manuellement par le SCG basé sur l'image RSO correspondante de même que d'autres données auxiliaires pour fournir des informations sur les concentrations de glaces, les types de glaces ainsi que la dimension des floes à l'intérieur de régions délimitées par des « polygones ». Le système MAGIC utilise ces informations comme données d'entrée et génère ensuite une carte à l'échelle du capteur (basée sur le pixel) pour chaque polygone, un produit trop coûteux à produire manuellement. La caractéristique principale de la présente version 1.0 du système MAGIC est l'ajout d'un module de segmentation qui a été évalué avec succès sur un certain nombre d'images. MAGIC est conçu non seulement pour être utilisé comme outil spécifique d'interprétation de la glace de mer, mais également comme plate-forme générale pour l'interprétation des images numériques génériques en ayant recours aux algorithmes fondamentaux et avancés qui y sont intégrés.
[Traduit par la Rédaction]

Introduction

The automated interpretation of digital imagery is a complex, challenging task in computer vision. The application of this technology to remote sensing has been an ongoing research endeavor since satellite imagery was first obtained and has become more important with the increased volume of imagery captured by a myriad of satellites. The objective is to automatically apply the following tasks in order to the digital imagery: segment (break image into distinct, uniform regions), cluster (group like regions), and classify (assign class labels to regions).

MAp-Guided Ice Classification (MAGIC) is a software system designed and built to interpret digital imagery. Its primary mandate is to interpret operational synthetic aperture radar (SAR) imagery but has been implemented to facilitate interpretation of other remote sensing imagery and any generic digital imagery. The research represents the amalgamation of many years of published research into a cohesive, usable framework. This was necessitated for two reasons. First, multiple contributors have worked independently to develop algorithms and, as such, there was no means of directly comparing various algorithms on the same platform. Also, without algorithm integration, some domain knowledge was being lost with the natural departure of graduate students and postdoctoral fellows. Second, algorithms were built without any integration with user-friendly visualization tools to properly and efficiently process data and analyze the results. This made it very difficult to run tests and compare results quantitatively and qualitatively. Both of these reasons motivated an operational and research tool that has the potential to be used by other scientists as well to compare standard and state-of-the-art image interpretation techniques.

MAGIC is an ongoing research endeavor, and version 1.0 is described in this paper. MAGIC is unique in that it can interpret SAR sea ice imagery using accompanying operational ice charts. MAGIC uses operator-provided polygons in the ice chart as a starting point to interpret ice types on a per-pixel basis. This will lead to better comprehension of the ice situation within any particular polygon and provide a more precise estimate of ice type concentrations. MAGIC is

Received 23 December 2007. Accepted 3 June 2009. Published on the Web at http://pubservices.nrc-cnrc.ca/cjrs on 16 July 2010.

D.A. Clausi,[1] A.K. Qin,[2] M.S. Chowdhury, and P. Yu. Systems Design Engineering, University of Waterloo, Davis Centre 2599, Waterloo, ON N2L 3G1, Canada.

P. Maillard. Universidade Federal de Minas Gerais, Belo Horizonte MG, Brazil.

[1]Corresponding author (e-mail: dclausi@uwaterloo.ca).

[2]Corresponding author (e-mail: qfred008@gmail.com).

not constrained by the ice chart information. For any digital imagery, users can specify the number of classes and draw custom polygons, which enables users to independently interpret any part of the image. MAGIC version 1.0 is featured with its segmentation module, which utilizes only intensity information as a feature to perform image segmentation. Its validity has been evaluated on many SAR and generic images.

Background

Sea ice monitoring and mapping are among the major operational applications of remote sensing technologies (Carsey, 1989). Sea ice affects operational and environmental activities including ship navigation, marine resource exploitation, and global climate monitoring. Timely and reliable sea ice information is important to facilitate these activities. SAR, as an active satellite microwave sensor, images extensive ice-infested ocean regions both day and night under all weather conditions (Hall, 1998).

SAR sea ice image segmentation is a challenging task due to the large variation of backscatter affected by environmental factors and sensor artefacts. The same ice type can have distinct appearances, and different ice types can have similar appearances with respect to different locations, seasons, or varying incident angles.

The Environment Canada Canadian Ice Service (CIS) personnel generate daily charts for ice-infested regions primarily using SAR imagery received from RADARSAT-1 and RADARSAT-2 satellites (www.asc-csa.gc.ca/eng/satellites/). Ice charts are essentially region-based ice distribution maps in which regions with visually homogeneous ice conditions are manually outlined as "polygons" and described by oval "egg code" symbols that summarize the ice characteristics of the region. An egg code contains numerical indices to depict the concentrations, types, and floe sizes of ice types inside a specific region, which adopts the World Meteorological Organization (WMO) standards (www.wmo.ch). **Figure 1** shows an egg code example, and a sample ice chart of the Gulf of St. Lawrence superimposed with egg codes is illustrated in **Figure 2**. A more detailed description can be found at the CIS Web site (http://ice-glaces.ec.gc.ca).

The standardized ice charts only contain regional information and do not provide at-sensor resolution information about the ice types within each polygon. It is desirable but not manually feasible to perform ice typing for individual pixels. Automated methods are preferred for pixel-level interpretation. This is the key motivator for the development of MAGIC.

Other research efforts have been devoted to developing SAR sea ice image interpretation systems. Haverkamp et al. (1993) introduced a dynamic local thresholding technique for three-category SAR sea ice image classification. Samadani (1995) proposed a finite mixture of gamma distributions model for estimating proportions of ice classes in a SAR image. A Multi-year Ice Mapping System (MIMS) (Fetterer and Ye, 1997) is used for rapid identification of high-latitude multiyear ice using a Fisher-criterion-based local thresholding method. Soh and Tsatsoulis (1999) described an automated SAR sea ice image segmentation system, characterized by dynamic local thresholding, multi-resolution peak detection, and aggregated population equalization spatial clustering. Soh et al. (2004) also built a system named Advanced Reasoning using Knowledge for Typing of Sea Ice (ARKTOS). ARKTOS performs image segmentation using a threshold-based watershed merging algorithm, generates a series of attribute descriptors for the segments, and then uses expert rules (Dempster–Shafer theory) drawn from a knowledge database to classify each segment. Karvonen (2004) developed a SAR sea ice image classification system based on a modified Pulse-Coupled Neural Network (PCNN). Most of these methods cannot support general sea ice segmentation and classification in the context of various ice types, speckle noise, different seasons, and geographical locations of sea fields due to the challenging nonstationary properties of the SAR sea ice imagery.

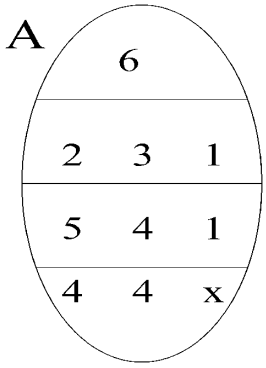

Figure 1. Example of an egg code. The letter "A" denotes the label of the region. The first row indicates that the total ice concentration is 60%, the second row indicates the individual concentrations for each ice type (thickest to thinnest, from left to right), the third row shows a coding for the ice type, and the last row indicates the floe size of each ice component ("x" in the last row denotes no ice or undetermined floe size).

The basis of this research has been provided by prior publications from the MAGIC research group. Various texture feature extraction approaches applied to SAR sea ice images have been investigated, improved, and compared (Clausi and Jernigan, 1998; 2000; Clausi, 2001; Deng and Clausi, 2004a). Novel image segmentation and classification methods have been devised to effectively interpret the SAR sea image imagery (Deng and Clausi, 2005; Yu and Clausi, 2005). Two techniques emphasizing the classification task are presented in Yu and Clausi (2005) and Maillard et al. (2005). To have a unified system to encapsulate these algorithms and allow visual assessment of the results is desirable. The MAGIC system has been designed to achieve this goal.

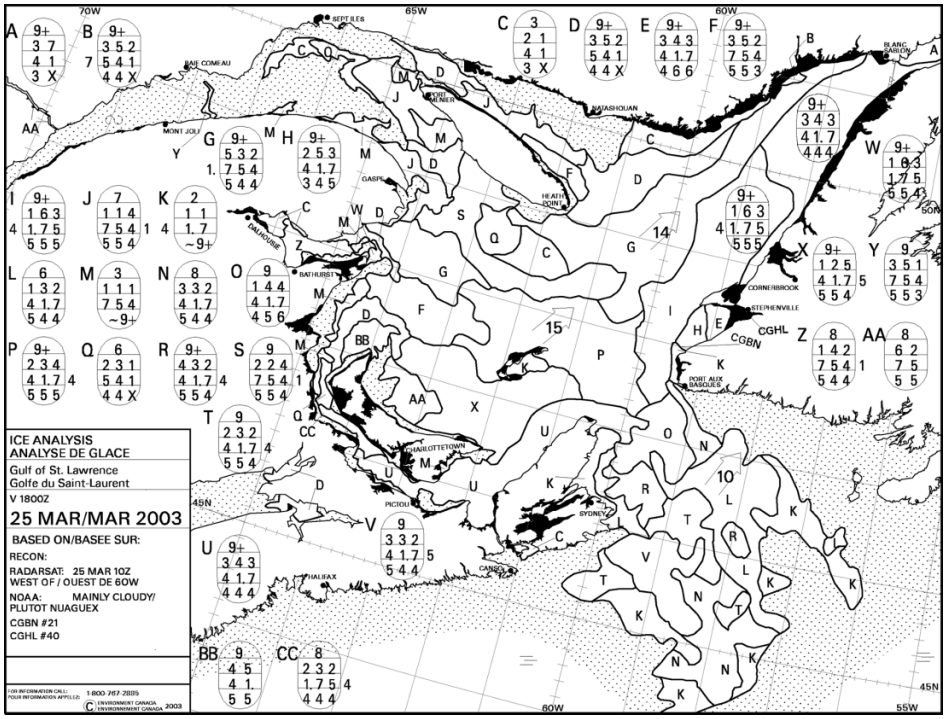

Figure 2. An ice chart example from the CIS Web site (http://ice-glaces.ec.gc.ca).

MAGIC version 1.0 system

Overview

MAGIC is built in C++ under the Microsoft .NET 2.0 framework. A schematic representation of the MAGIC version 1.0 system architecture is shown in **Figure 3**. In MAGIC version 1.0, a user-friendly graphical user interface (GUI) coordinates data input/output (I/O), visualization, and operations. These components are described in this section.

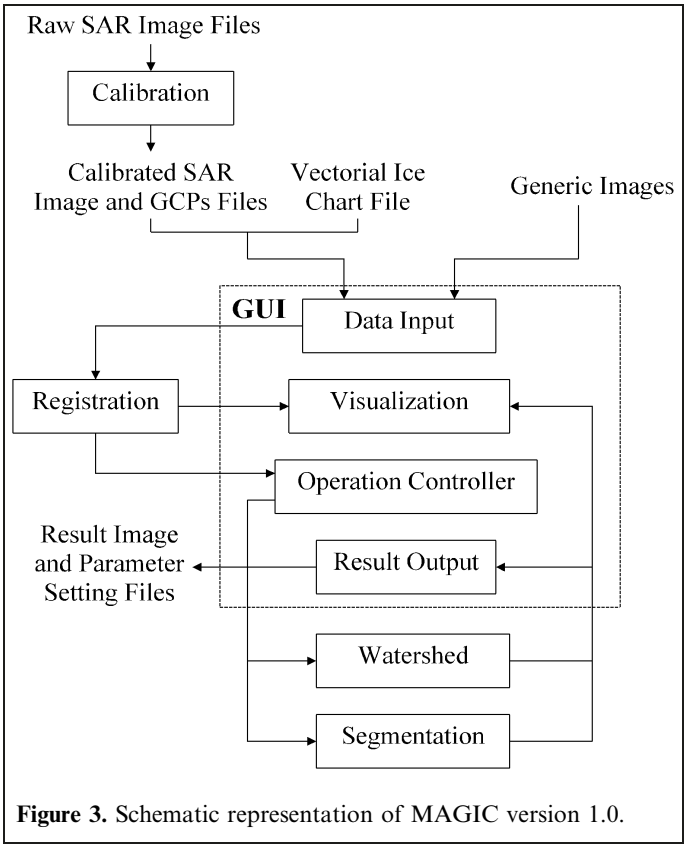

Figure 3. Schematic representation of MAGIC version 1.0.

Navigating the GUI

The MAGIC GUI is shown in **Figure 4** and displays all polygons depicted in the ice chart with visible white boundaries overlaid on the SAR image scene. A listing of the polygons, by polygon number, is found in the polygon selection scrollbar at the top right. By clicking a listed polygon, the corresponding polygon region is outlined in red and its associated egg code data are displayed at the bottom right. Correspondingly, by double-clicking within a polygon region, the corresponding polygon in the polygon selection scrollbar is highlighted and the corresponding egg code is presented. The zooming tool and mouse can be used to change the image resolution. The image can be panned by clicking, holding, and dragging the mouse.

Various tasks can be performed by following the menu items File, View, Setup, Watershed, Segmentation, and Help. Some general information related to the current image such as image directory, image size, coordinate of the current mouse cursor location, and the total polygon number in the image is displayed in the title and status bars. The size of the SAR image being processed in **Figure 4**

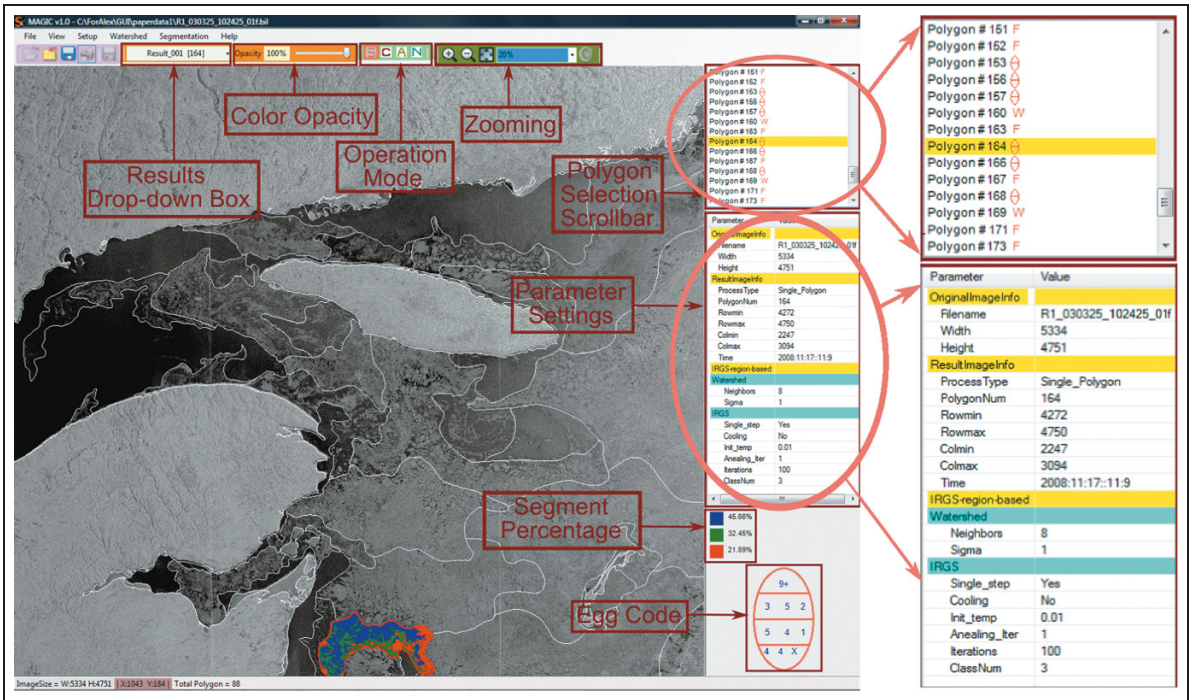

Figure 4. Screen shot of the GUI of MAGIC version 1.0.

is 5334 pixels × 4751 pixels (2 × 2 block average (Bertoia and Ramsay, 1998) of the original ScanSAR wide image at resolution 100 m and pixel spacing 50 m) and contains 88 polygons.

Input and output files

The CIS provides raw RADARSAT-1 ScanSAR wide-mode image files in the .avg format (Bertoia and Ramsay, 1998) along with their accompanying ice chart vector data files in the .txt format. The .avg image files contain SAR sensing parameters, raw image values, and ground control points (GCPs), which cannot be directly used by MAGIC. The ice chart vector data file contains geocoding information for outlines of polygons within the corresponding SAR image scene and egg code information.

A separate calibration program has been built to produce input files for MAGIC from the .avg files. It compensates for varying incident angles and transforms image values into backscattering coefficients. After black image borders are cropped, backscattering coefficients are stored in a .bil file according to the "band-interleaved-by-line" structure. In addition, the program extracts GCPs and their associated image Cartesian coordinates from the .avg files and save them in a .txt file. The obtained .bil image file and .txt GCPs file are used together with the ice chart vector data file as input to MAGIC. In fact, MAGIC can also directly take generic bitmap images as input.

Any image segmentation result generated by MAGIC can be saved in the .bil or .bmp format for future viewing. Algorithmic parameter settings related to that result are recorded in an .xml file for future reference.

Data preprocessing

The CIS ice chart vector data file describes the profile of each polygon using a set of latitude–longitude coordinates. Registration is required to overlay polygons onto the corresponding SAR image scene in the Cartesian coordinate system. A Lambert Conformal Conic (LCC) projection (Snyder, 1987) using the Canadian North American datum for 1927, followed by a polynomial fitting (Press et al., 1992) with parameters determined via available pairs of the GCP and the image Cartesian coordinate, is applied to convert geographical coordinates of polygon profiles to Cartesian coordinates. A raster mask map is then produced in which each registered polygon is filled with its polygon number from the ice chart file. For segmentation, the total number of classes is provided by the egg code information, which equals the number of ice types indicated in the egg code plus open water if the total concentration is less than 9+.

Generic digital imagery (remote sensing or otherwise) is read without any ancillary information, and the number of classes is set by the user.

Watershed

A watershed (Vincent and Soille, 1991) is a stand-alone algorithm that segments an entire image into regions with closed boundaries. When applied to natural imagery, especially noisy SAR imagery, the watershed algorithm over-segments, which means that the algorithm partitions an image into numerous small regions. The algorithm by Vincent and Soille (1991) is implemented in MAGIC.

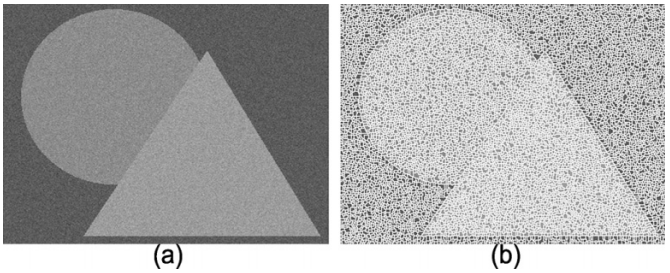

Figure 5. Watershed segmentation example on a synthetic image: (a) synthetic image (279 × 378 pixels); (b) watershed segmentation result.

In MAGIC, the over-segmented result is used as an initialization for region-based segmentation, which involves an iterative approach for merging and clustering regions (Yu and Clausi, 2005; 2008). Segmentation techniques using watershed regions instead of individual pixels as the processing unit significantly reduce computational demands.

Figure 5 shows the segmentation result by applying the watershed algorithm to a synthetic image of size 279 × 378 pixels. This image is generated by adding Gaussian noise of mean 0 and standard deviation 10 to a clean image composed of three grey levels, namely 96, 144, and 160. A total of 10 338 closed regions are generated, separated by white boundaries.

Segmentation process

The segmentation method is selected via the menu item, and pop-up windows allow for algorithm parameters to be modified. Segmentation can be performed using either individual pixels or regions generated by the watershed algorithm as a starting point. For regions, a region adjacency graph (RAG) structure (Li, 2001) is constructed from the over-segmented watershed regions. Each node in the RAG represents a watershed region, and links between nodes denote the common boundaries between neighboring watershed regions. The segmentation approach is then formulated on the RAG instead of the regular image lattice.

MAGIC provides four different operation modes for segmentation processing: (*i*) single-polygon mode allows segmentation on a selected polygon created by an ice map; (*ii*) custom-polygon mode allows segmentation on a single user-drawn polygon; (*iii*) all-polygons mode sequentially segments all polygons created by an ice map in a whole SAR scene; and (*iv*) no-polygon mode segments full images, SAR or otherwise.

The algorithm progress is displayed in the status bar located at the bottom of the GUI, as shown in **Figure 4**. The segmentation result is displayed in the viewing window where each polygon region displays distinctly colored segments. Color opacity can be adjusted via the opacity toolbar, so users can effectively evaluate the result and simultaneously view the SAR scene details. Segment percentages and algorithmic parameter settings leading to that segmentation result are shown at the bottom right and can be optionally saved. The results drop-down box is used for viewing previously saved results for that image.

Among the existing image segmentation methods, the Markov random field (MRF) model based segmentation algorithms (Li, 2001; Panjwani and Healey, 1995; Deng and Clausi, 2004b; 2005; Yu and Clausi, 2005; 2008) have shown promising performance for SAR imagery. In the MRF model, the spatial context is taken into account by formulating the local interactions among neighboring pixels. The segmentation module in MAGIC contains the following methods: K-means (Duda et al., 2000), Gaussian mixture model (Duda et al., 2000), constant multilevel logistic (MLL) model (Li, 2001), variable MLL model (Deng and Clausi, 2004b; 2005), graduated increased edge penalty (Yu and Clausi, 2008), and iterative region growing with semantics (IRGS) (Yu and Clausi, 2005; 2008). The method that acts as our state-of-the-art approach is IRGS,which combines the attractive features of edge-based and region-growing-based segmentation methods.

Segmentation examples

Segmentation tests are presented of single, custom, all, and no polygons using two RADARSAT-1 SAR sea ice images, one RADARSAT-1 SAR wetland image, and one synthetic image. The IRGS algorithm is used exclusively for example purposes using only backscatter as a feature. Algorithmic parameters are fixed for all cases ($C_1 = 5$ and $C_2 = 0.4$ for β adjustment, and the total number of iterations is set to 100). Since MAGIC version 1.0 does not provide automatic ice type labeling, we manually assign an ice type or open water to each segmented region.

Quantitative validation of segmentation results ideally requires corresponding sensor-resolution ground truth. However, provision of sensor-resolution validation field or manually segmented data for SAR sea ice imagery is not feasible. Operationally, classification using WMO standards on a regional basis involves years of experience of sea ice experts, and this is the base data that we are utilizing. For the purposes of this research, an arms-length senior SAR sea ice expert from the CIS carefully analyzed all SAR segmentations presented in this paper and confirmed the accuracy of these segmentations as well as the ice types that were assigned to individual segments. In addition, a test is provided using a synthetic imagery with known ground truth.

Segmentation of single polygons

Tests are based on single polygons derived from operational ice maps. Two operational SAR sea ice images with associated ice maps are used. The first image, as shown in **Figure 6a**, was captured on 25 March 2003 over the Gulf of St. Lawrence and has dimensions 5334 × 4751 pixels. The second image, as shown in **Figure 6b**, was captured on

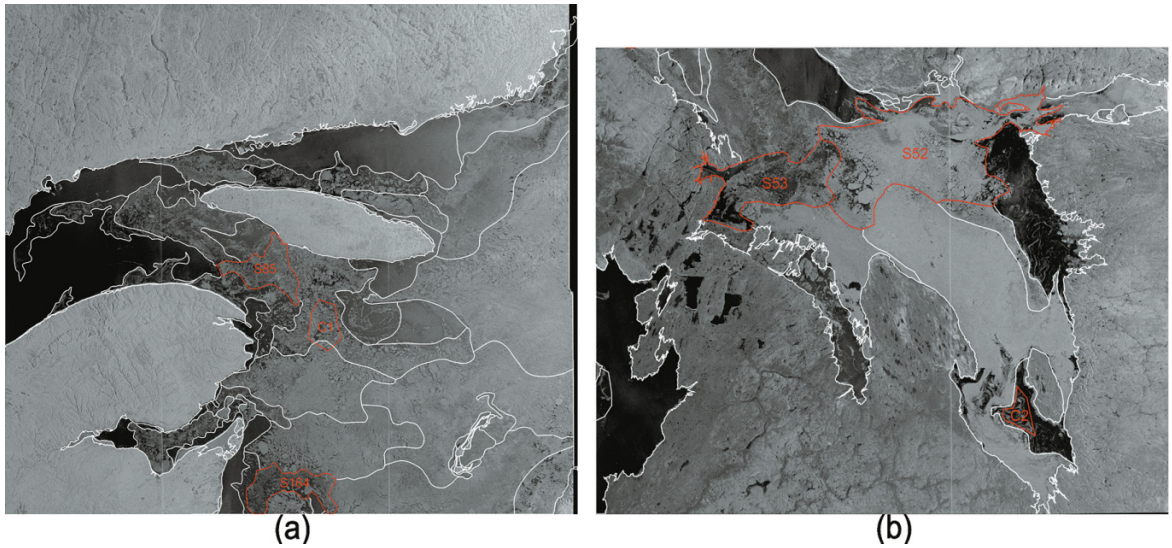

Figure 6. Two operational SAR sea ice images with associated ice chart polygons. (a) SAR image (5334 × 4751 pixels) captured on 25 March 2003 over the Gulf of St. Lawrence. S85 and S164 represent two single polygons numbered 85 and 164, respectively. C1 represents a user-defined custom polygon. (b) SAR image (4688 × 3818 pixels) captured on 6 October 2004 over the Gulf of Boothia (within the Canadian Arctic). S52 and S53 represent two single polygons numbered 52 and 53, respectively.

6 October 2004 over the Gulf of Boothia (within the Canadian Arctic) and has dimensions 4688 × 3818 pixels. Both images are obtained via 2 × 2 block average (Bertoia and Ramsay, 1998) of the original ScanSAR wide image at resolution 100 m and pixel spacing 50 m. Two polygons from each scene are tested, namely S85 and S164 highlighted in **Figure 6a** and S52 and S53 highlighted in **Figure 6b**. Image segmentation results are presented in **Figures 7**, **8**, **9**, and **10**. Egg codes and segmented ice type concentrations are presented in **Table 1**.

Figure 7 shows the segmentation of polygon S85. Three levels of opacity are displayed for this example. **Figure 7b** shows the segmentation at zero opacity (only boundaries are displayed), **Figure 7c** shows partial opacity, and **Figure 7d** shows full opacity. This tool easily allows a user to evaluate the quality of the segmentation by varying the opacity to view segmented regions and SAR backscatter simultaneously. The three segmented regions are characterized by darker signatures with about 11% concentration, ice fractures with about 45% concentration, and brighter consolidated appearances with about 44% concentration. Since ice floe information provided by the corresponding egg code indicates the same floe sizes for grey-white ice and grey ice and no floes for new ice, floe size is not useful for distinguishing grey-white ice and grey ice. As shown in **Table 1**, the segmentation results do not match the egg code concentrations.

The three segmented regions with respect to polygon S164 as shown in **Figure 8** have visual properties similar to those of polygon S85. **Table 1** gives the ice labeling result on the segmented regions. Grey ice (46%) is identified with similar concentrations as indicated in the egg code, but new ice (32%) has a higher percentage, and grey white ice (22%) has a lower percentage.

In the segmentation maps of polygon S52 shown in **Figure 9**, the region having a bright consolidated appearance with large ice floes is identified as multiyear ice (54%) and the region having a relatively darker appearance than the multiyear ice region is identified as second-year ice (24%). Here, the floe size information provided in the associated egg code is used as a clue to visually distinguish multiyear and second-year ice. The region having the darkest appearance is identified as open water (12%), and the region with relatively brighter signatures than the open water region is identified as new ice (10%). **Table 1** summarizes this ice labeling result, which resembles the egg code concentrations.

In the segmentation maps of polygon S53 shown in **Figure 10**, the ice floe information is not useful in the ice type assignment because multiyear ice and grey ice have the same floe sizes, and new ice and open water do not contain ice floes. The region containing bright consolidated contents is identified as multiyear ice (22%). Grey ice is assigned to the region having several dark ice fractures (37%). New ice is assigned to the region with the darkest appearance (9%). The region having brighter textures on a dark background is identified as wind-roughened open water (32%). This result is described in **Table 1** and does not closely match the egg code concentrations.

For both polygons S52 and S53, total ice concentrations produced with MAGIC are less than those given in the egg codes, which indicates a tendency of overestimation of the total ice concentration in egg codes. It is also worth noting that there is an island (Crown Prince Federik Island) on the

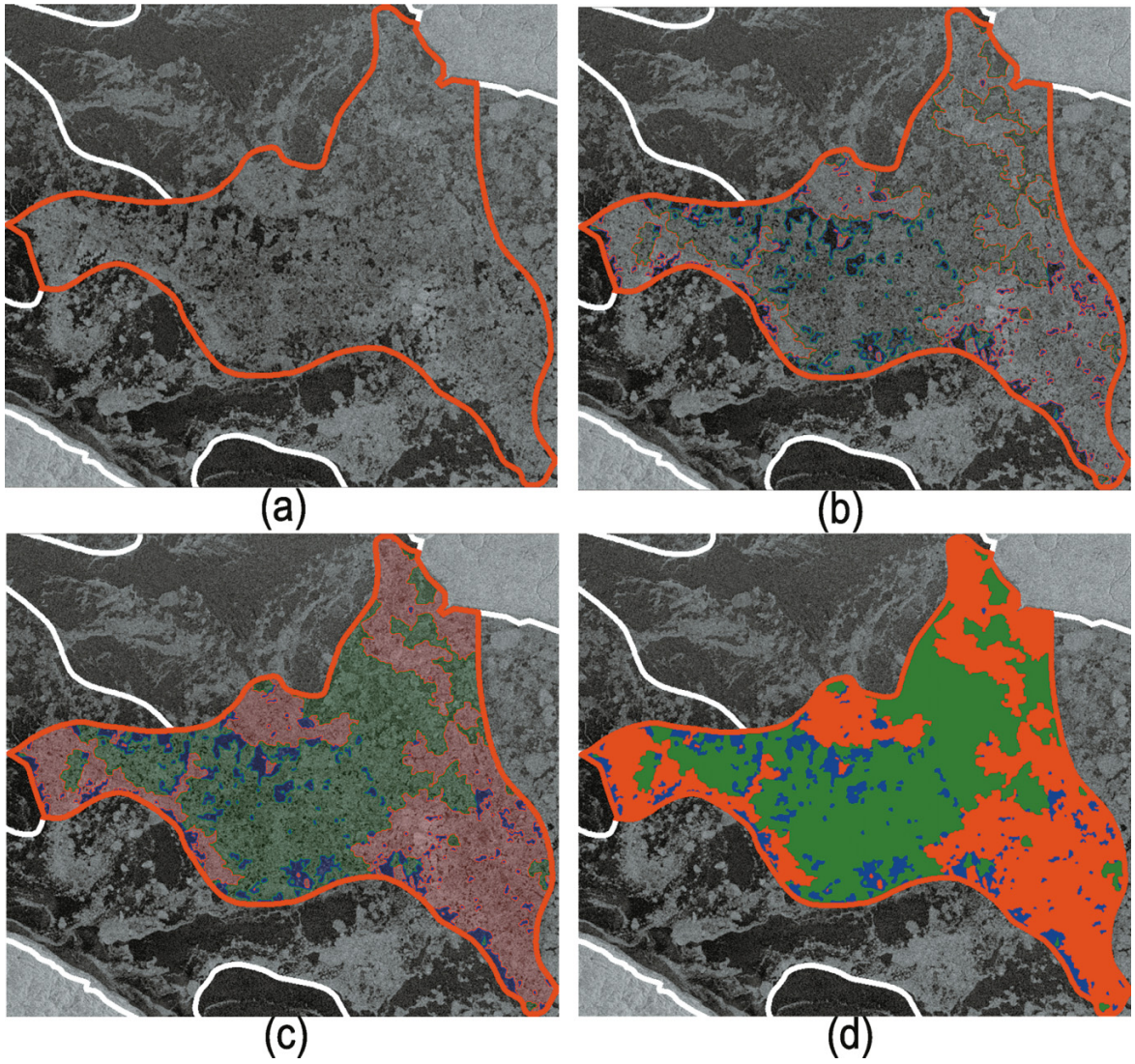

Figure 7. Segmentation result on single polygon S85 in the Gulf of St. Lawrence image. Red regions represent grey-white ice, green regions grey ice, and blue regions new ice. (a) Single polygon S85. (b) Segmentation map at zero color opacity. (c) Segmentation map at partial color opacity. (d) Segmentation map at full color opacity.

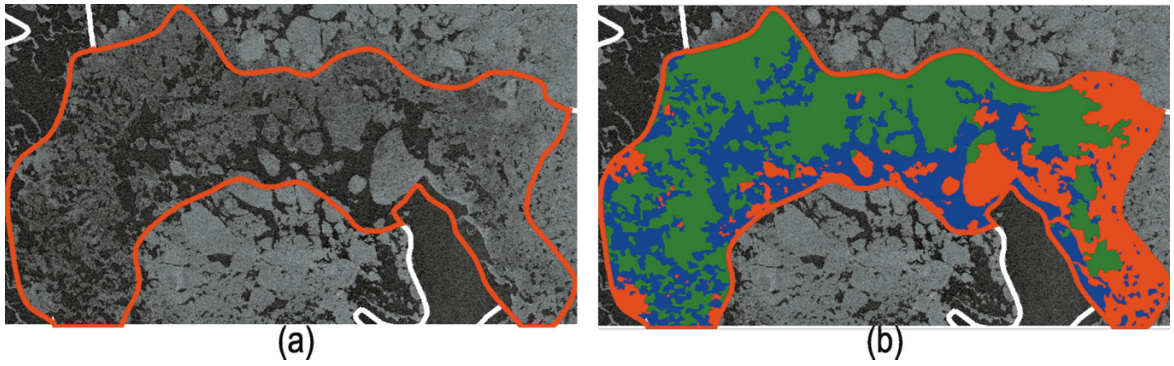

Figure 8. Segmentation result on single polygon S164 in the Gulf of St. Lawrence image. Red regions represent grey-white ice, green regions grey ice, and blue regions new ice. (a) Single polygon S164. (b) Segmentation map at full color opacity.

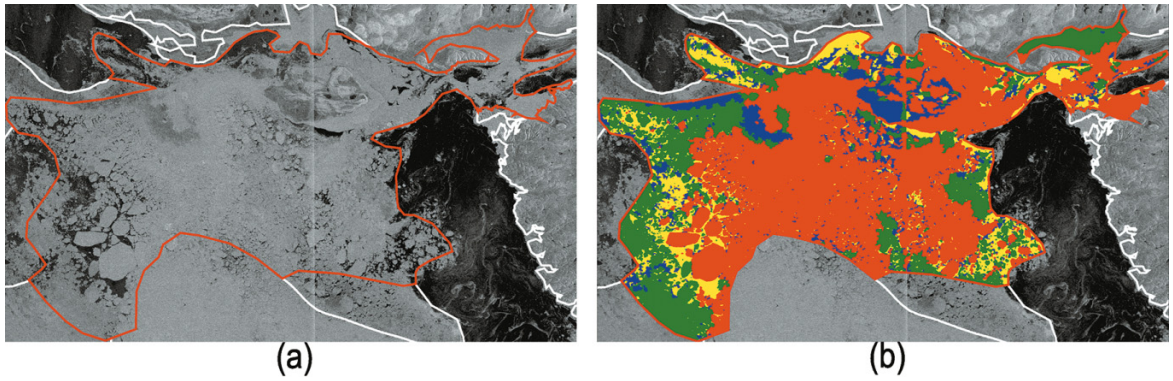

Figure 9. Segmentation result on single polygon S52 in the Gulf of Boothia image. Red regions represent multiyear ice, green regions second-year ice, blue regions new ice, and yellow regions open water. (a) Single polygon S52. (b) Segmentation map at full color opacity.

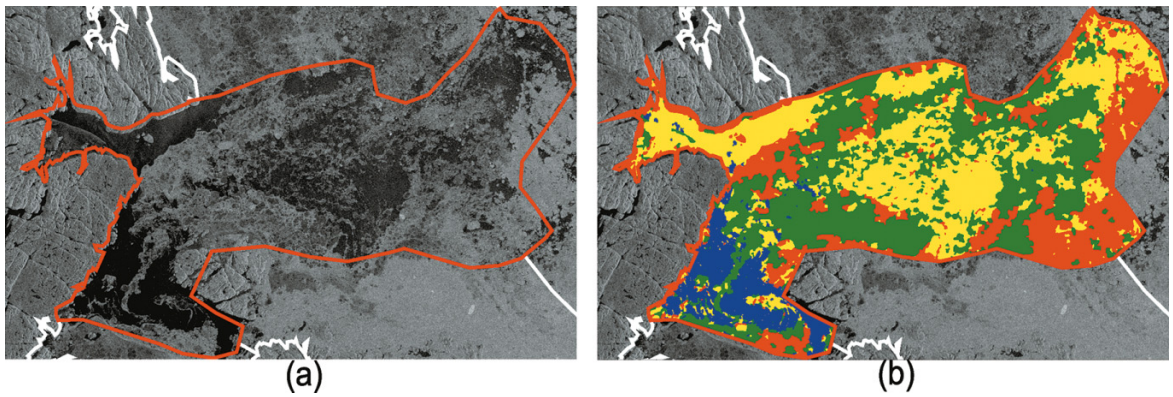

Figure 10. Segmentation result on single polygon S53 in the Gulf of Boothia image. Red regions represent multiyear ice, green regions grey ice, blue regions new ice, and yellow regions open water. (a) Single polygon S53. (b) Segmentation map at full color opacity.

Table 1. Comparative analysis of egg code derived ice concentrations with concentrations produced with MAGIC.

	Multiyear ice	Second-year ice	Grey-white ice	Grey ice	New ice	Open water
Figure 7						
Egg code (%)	—	—	20	60	20	—
Segmentation (%)	—	—	44	45	11	—
Figure 8						
Egg code (%)	—	—	30	50	20	—
Segmentation (%)	—	—	22	46	32	—
Figure 9						
Egg code (%)	50	30	—	—	10	10
Segmentation (%)	54	24	—	—	10	12
Figure 10						
Egg code (%)	10	—	—	40	30	20
Segmentation (%)	22	—	—	37	9	32

Note: Two polygons are used for each of two operational SAR images. —, ice type not present in that polygon.

top right of polygon S52 which is not described in the CIS vector ice chart. Since MAGIC relies on this ice chart file to perform segmentation, it cannot avoid partitioning this island. A similar case happens for polygon S53, in which islands (bottom left) are not included in the ice chart. In addition, the ice chart does not continuously approximate

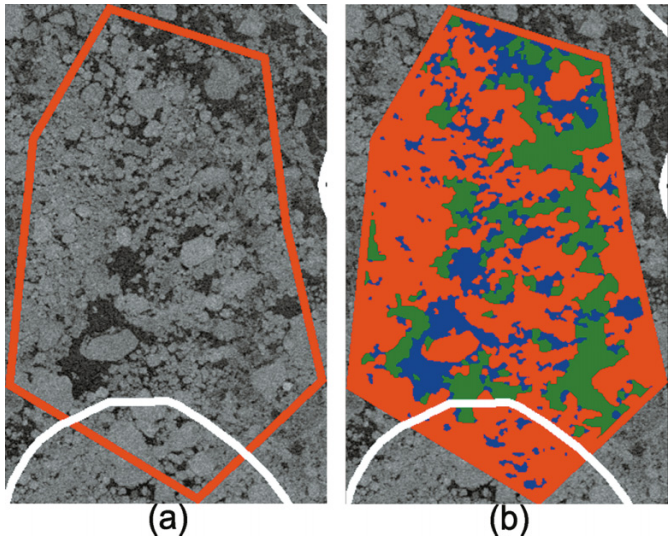

Figure 11. Segmentation result on custom polygon C1 in the Gulf of St. Lawrence image. Red regions represent thin first-year or grey-white ice, green regions grey ice, and blue regions new ice or open water. (a) Customized polygon C1. (b) Segmentation map at full color opacity.

the coastline (top left). Again, MAGIC produces a visually meaningful segmentation result. Segmentation results obtained by MAGIC with an inaccurate vector ice chart will inevitably misrepresent ice concentrations.

There are various potential sources of error responsible for the mismatch between ice concentrations obtained in segmentation and those given in egg codes as shown in **Table 1**. Ice analysts work in a real-time production environment with limited time to visually interpret and label an image. Although their ability to type and classify ice is considerable, their ability to accurately and consistently estimate concentration over polygons is subject to human error, as per feedback from CIS personnel, and is estimated to be in the range of 10%–20% (10% in high-concentration regimes). In addition, ice analysts may use a variety of ancillary information not present in the SAR scene to make an assessment, and this information is not available to the automated segmentation algorithm.

Segmentation of custom polygons

In custom polygon mode, the user can draw a closed boundary around any area of interest within the image and then segment that region. Here, a custom polygon C1 is highlighted in **Figure 6a** with the segmentation result shown in **Figure 11**. Three classes are specified, and these are characterized by dark signatures representing open water or new ice (17%, shown in blue), grey ice fractures with a brighter background (24%, shown in green), and bright more consolidated floes representing thin first-year ice or grey-white ice (55%, shown in red).

Segmentation of all polygons

The all-polygon mode segments each polygon in the scene independently. **Figure 12** displays the segmentation maps for **Figure 6** at full color opacity. Each color inside each polygon denotes a particular ice type for that polygon. The ability to cluster like ice types across all polygons in the scene and assign a common color label to each ice type is not yet included in the MAGIC package. There is no definitive technique to do this; however, future MAGIC releases are expected to include such a technique. One such

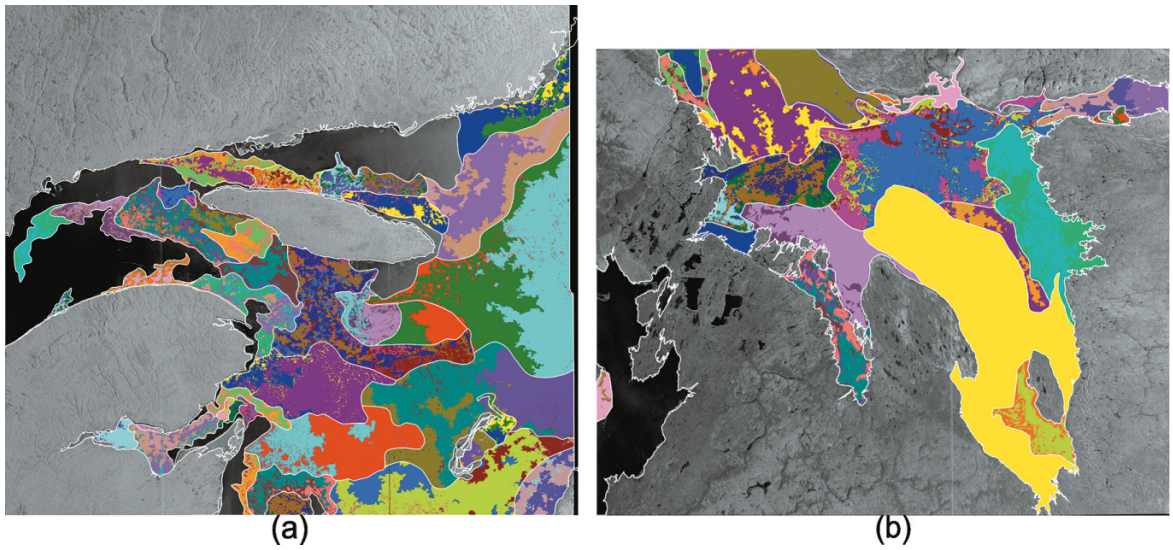

Figure 12. Segmentation result on all polygons of two operational SAR sea ice images. (a) All-polygons segmentation map of the Gulf of St. Lawrence image. (b) All-polygons segmentation map of the Gulf of Boothia image.

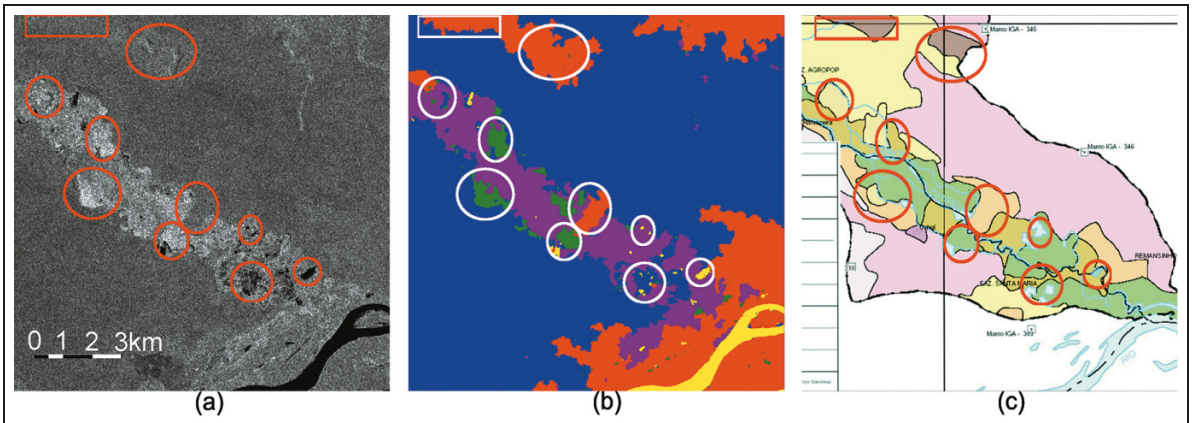

Figure 13. Segmentation result on the Pandeiros wetland image with validation map. In the segmentation map, red regions represent high mesophilous forest, blue regions woody savanna and agriculture on dry soils, purple regions shrub wetlands, green regions herbaceous wetlands, and yellow regions open water. (a) SAR image (1024 × 1024 pixels at nominal resolution 12.5 m) captured in April 2004 over Pandeiros wetland. (b) Segmentation map. (c) Validation map.

labeling technique developed by the group is the cognitive reasoning approach (Maillard et al., 2005), and various methods are under current investigation.

Segmentation without polygons

To validate the efficacy of MAGIC version 1.0 on segmenting generic images other than sea ice, we use one RADARSAT-1 S2 mode image of a wetland region in Brazil (**Figure 13a**). This image was acquired in April 2004 with supporting validation data. The region of interest is part of a large wetland area (~3500 ha) known as Pandeiros (15°40′ south, 44°38′ west) considered as having extreme ecological importance due to its situation in a semiarid savanna region. Due to its short-wavelength (C-band) and HH copolarization configuration, RADARSAT-1 data are not well suited for broad-leaf forest. Conversely, it has shown good potential for mapping flooded vegetation, especially wetlands dominated by herbaceous vegetation (Deng and Clausi, 2001).

Without prespecified polygons, segmentation is applied to the entire scene with the result shown in **Figure 13b**. In this segmentation map, the five colors can be interpreted as follows: high mesophilous forest are in red (the northern sections represent leaf-on deciduous forests on limestone rock, whereas the larger southern part represents riparian forest on fluvial sediments), woody savanna and agriculture on dry soils are in blue, shrub wetlands appear in purple, herbaceous wetlands are in green, and open water is in yellow. The main structures and a number of small elements (outlined in white) have direct correspondence with those in the validation map (**Figure 13c**).

The capability of MAGIC to segment generic imagery is also demonstrated using the synthetic image in **Figure 5**. The segmentation map shown in **Figure 14** indicates that the three grey levels behind the noise can be well separated as individual regions. The fairly small segmentation error (0.2%) calculated based on the available validation image verifies the segmentation accuracy.

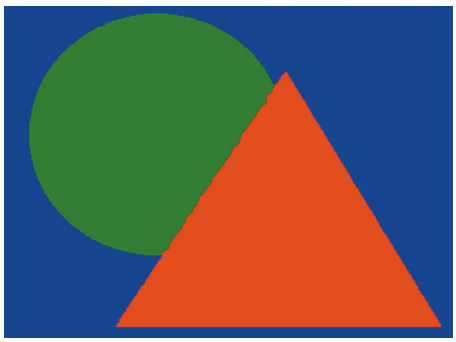

Figure 14. Segmentation result on the synthetic image in **Figure 5**.

Table 2 reports the running time of the segmentation algorithm on all of the test images. With larger polygons, there is an exponential increase in computational time due to the increased time and memory involved in storing and using the region adjacency graph (RAG) (Li, 2001). Pixel-based segmentation approaches do not require a RAG because the image is stored in a raster format. In the early stages of the IRGS algorithm, there are many regions to consider, and this can be very time consuming. Segmentation of all polygons in each scene is completed within an hour, which verifies the operational usage of MAGIC.

Future development

MAGIC version 1.0 has demonstrated robust image segmentation for SAR imagery. New features will be incorporated to derive future MAGIC versions. **Figure 15** illustrates the architecture of the future system.

Table 2. Running time of the segmentation algorithm on all of the test images.

Polygon	Segmentation time (s)
Gulf of St. Lawrence (Figure 6a)	
S85	23
S164	25
C1	8
All	3250
Gulf of Boothia (Figure 6b)	
S52	349
S53	35
All	890
Pandeiros wetland (Figure 13a)	
None	823
Synthetic image (Figure 5a)	
None	35

Note: Tests were performed on a Windows Vista PC with an AMD 2.3 GHz dual-core central processing unit (CPU) using 2 gigabytes of memory.

(1) To reach a broader audience, MAGIC needs to be able to support other remote sensing and generic image formats.

(2) MAGIC version 1.0 can only process univariate features. Future MAGIC releases will be multivariate to handle multipolarized SAR data, color images, texture features, and multispectral remote sensing images.

(3) MAGIC will support RADARSAT-2 dual-polarization imagery, since the CIS intends on using both HH and HV bands for operational analysis. The HV band is expected to provide improved open water recognition (Ramsay et al., 2004). The research effort involves the best means to combine these two bands to optimize joint segmentation capability.

(4) MAGIC will incorporate texture extraction methods to augment the backscatter feature. Texture analysis has had a long history in the analysis of SAR sea ice imagery, but its operational use has never been fully realized. Existing routines for co-occurrence, Gabor, and MRF texture feature extraction methods (Clausi and Jernigan, 1998; 2000; Clausi, 2001; Deng and Clausi, 2004a) will be integrated.

(5) MAGIC will incorporate an edge-preserving denoising module (Tomasi and Manduchi, 1998; Yang and Clausi, 2007). Denoising as a preprocessing step for the watershed algorithm that retains edge content will minimize the number of watershed regions generated and, in turn, dramatically reduce the time required for segmentation.

(6) The future MAGIC system will contain linear or nonlinear dimensionality reduction methods (Liu and Motoda, 1998), which can be applied to generate a low-dimensional feature set that retains the important properties of the original image. This is desirable to improve performance and speed of the subsequent operations.

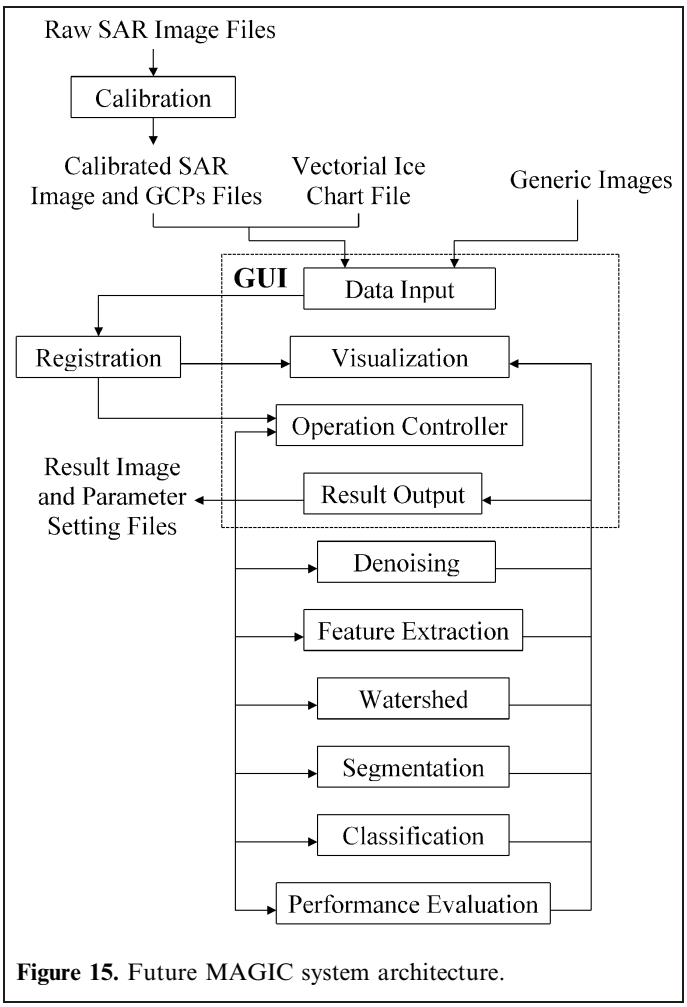

Figure 15. Future MAGIC system architecture.

(7) Although application of algorithms to operational imagery is required, for research and development purposes, being able to generate artificial SAR sea ice imagery where the ice class of each pixel is known would be useful (Wong et al., 2009).

(8) MAGIC will incorporate a classification module. Segmented regions can be assigned to a class based on prior information (Yu and Clausi, 2005; Maillard et al., 2005). For SAR sea ice image interpretation, pixel-based ice labeling is the ultimate goal, so including this capability is critical.

(9) In cases where validation data are available, MAGIC will apply a performance evaluation module.

Conclusions

The MAGIC is a system designed for the automated interpretation of operational SAR sea ice imagery. In

addition, the system has been extended to allow for the interpretation of any generic digital image. MAGIC includes an easy-to-use GUI for segmenting digital images and studying the results. For operational SAR imagery, individual, all, or custom polygon regions can be processed using state-of-the-art and traditional segmentation routines. Future versions of MAGIC will expand and enhance the current functionality, especially with consideration to dual-polarization RADARSAT-2 imagery.

For SAR sea ice image interpretation, whether polygon, full-scene, or subscene based, MAGIC will effectively produce a sensor-resolution segmentation, a task not realistically performed by a human. For the purposes of environmental monitoring, large regions over multiple dates can be studied for ice type and open-water concentrations, improving the local understanding of ice shrinkage in polar regions. For the purposes of shipping routes, MAGIC can be used to study local regions and ascertain fairly precise locations of thinner ice that would be preferred for ship navigation. These are important considerations, given the world-wide concern of global warming and the costs and risks associated with ships breaking ice unnecessarily.

Acknowledgements

Funding for this project was provided by a Natural Sciences and Engineering Research Council of Canada (NSERC) discovery grant, the Canadian Federal International Polar Year (IPY) project, and Geomatics for Informed Decisions (GEOIDE; www.geoide.ulaval.ca/). We specifically thank Dr. Roger De Abreu at the CIS for segmentation validation and valuable comments. Thanks is extended to various CIS personnel for support and ongoing data provision.

References

Bertoia, C., and Ramsay, B. 1998. Sea ice analysis and products: cooperative work at the U.S. and Canadian national ice centers. In *IGARSS'98, Proceedings of the IEEE International Geoscience and Remote Sensing Symposium*, 6–10 July 1998, Seattle, Wash. IEEE, New York. pp. 1944–1947.

Carsey, F. 1989. Review and status of remote sensing of sea ice. *IEEE Journal of Oceanic Engineering*, Vol. 41, No. 2, pp. 127–138.

Clausi, D.A. 2001. Comparison and fusion of co-occurrence, Gabor, and MRF texture features for classification of SAR sea ice imagery. *Atmosphere and Oceans*, Vol. 39, No. 4, pp. 183–194.

Clausi, D.A., and Jernigan, M.E. 1998. A fast method to determine co-occurrence texture features. *IEEE Transactions on Geosciences and Remote Sensing*, Vol. 36, No. 1, pp. 298–300.

Clausi, D.A., and Jernigan, M.E. 2000. Designing Gabor filters for optimal texture separability. *Pattern Recognition*, Vol. 33, No. 11, pp. 1835–1849.

Deng, H., and Clausi, D.A. 2001. Mapping seasonal flooding in forested wetlands using multi-temporal RADARSAT SAR. *Photogrammetric Engineering & Remote Sensing*, Vol. 67, No. 7, pp. 857–864.

Deng, H., and Clausi, D.A. 2004a. Gaussian MRF rotation-invariant features for image classification. *IEEE Transactions on Pattern Analysis and Machine Intelligence*, Vol. 26, No. 7, pp. 951–955.

Deng, H., and Clausi, D.A. 2004b. Unsupervised image segmentation using a simple MRF model with a new implementation scheme. *Pattern Recognition*, Vol. 37, No. 12, pp. 2323–2335.

Deng, H., and Clausi, D.A. 2005. Unsupervised segmentation of synthetic aperture radar sea ice imagery using a novel Markov random field model. *IEEE Transactions on Geoscience and Remote Sensing*, Vol. 43, No. 3, pp. 528–538.

Duda, R.O., Hart, P.E., and Stork, D.G. 2000. *Pattern classification*. 2nd ed. Wiley-Interscience, Malden, Mass.

Fetterer, C.B., and Ye, J. 1997. Multi-year ice concentration from radarsat. In *IGARRS'97, Proceedings of the IEEE International Geoscience and Remote Sensing Symposium*, 3–8 August 1997, Singapore. IEEE, New York. pp. 402–404.

Hall, D. 1998. Remote sensing of snow and ice using imaging radar. In *Manual of remote sensing. Volume 2. Principles and applications of imaging radar*. Edited by F.M. Henderson and A.J. Lewis. 3rd ed. Wiley, New York. pp. 677–703.

Haverkamp, D., Soh, L.K., and Tsatsoulis, C. 1993. A dynamic local thresholding technique for sea ice classification. In *IGARRS'93, Proceedings of the IEEE International Geoscience and Remote Sensing Symposium*, 18–21 August 1993, Tokyo, Japan. Edited by S. Fujimura. IEEE, New York. pp. 638–640.

Karvonen, J.A. 2004. Baltic sea ice SAR segmentation and classification using modified pulse-coupled neural networks. *IEEE Transactions on Geoscience and Remote Sensing*, Vol. 42, No. 7, pp. 1566–1574.

Li, S.Z. 2001. *Markov random field modeling in computer vision*. 2nd ed. Springer-Verlag, New York.

Liu, H., and Motoda, H. 1998. *Feature extraction, construction and selection: a data mining perspective*. 1st ed. Springer, New York.

Maillard, P., Clausi, D.A., and Deng, H. 2005. Map-guided sea ice segmentation and classification using SAR imagery and a MRF segmentation scheme. *IEEE Transactions on Geoscience and Remote Sensing*, Vol. 43, No. 12, pp. 2940–2951.

Panjwani, D.K., and Healey, G. 1995. Markov random field models for unsupervised segmentation of textured color images. *IEEE Transactions on Pattern Analysis and Machine Intelligence*, Vol. 17, No. 10, pp. 939–954.

Press, W.H., Flannery, B.P., Teukolsky, S.A., and Vetterling, W.T. 1992. *Numerical recipes in C: the art of scientific computing*. 2nd ed. Cambridge University Press, Cambridge, U.K.

Ramsay, B., Flett, D., Andersen, H.S., Gill, R., Nghiem, S., and Bertoia, C. 2004. Preparation for the operational use of RADARSAT-2 for ice monitoring. *Canadian Journal of Remote Sensing*, Vol. 30, No. 3, pp. 415–423.

Samadani, R. 1995. A finite mixture algorithm for finding proportions in SAR images. *IEEE Transactions on Image Processing*, Vol. 4, No. 8, pp. 1182–1186.

Snyder, J.P. 1987. *Map projections — a working manual*. US Government Printing Office, Washington, D.C.

Soh, L.K., and Tsatsoulis, C. 1999. Unsupervised segmentation of ERS and radarsat sea ice images using multiresolution peak detection and aggregated population equalization. *International Journal of Remote Sensing*, Vol. 20, No. 15–16, pp. 3087–3109.

Soh, L.K., Tsatsoulis, C., Gineris, D., and Bertoia, C. 2004. ARKTOS: an intelligent system for SAR sea ice classification. *IEEE Transactions on Geoscience and Remote Sensing*, Vol. 42, No. 1, pp. 229–248.

Tomasi, C., and Manduchi, R. 1998. Bilateral filtering for gray and color images. In *Proceedings of the 6th International Conference on Computer Vision (ICCV'98)*, 4–7 January 1998, Bombay, India. Edited by S. Chandran and U. Desai. Narosa Publishing House, New Delhi, India. pp. 839–846.

Vincent, L., and Soille, P. 1991. Watersheds in digital spaces: an efficient algorithm based on immersion simulations. *IEEE Transactions on Pattern Analysis and Machine Intelligence*, Vol. 13, No. 6, pp. 583–598.

Wong, A., Zhang, W., and Clausi, D.A. 2009. Icesynth: an image synthesis system for sea-ice segmentation evaluation. In *Proceedings of the 6th Canadian Conference on Computer and Robot Vision (CVR 2009)*, 25–27 May 2009, Kelona, B.C. IEEE Computer Society, Los Alamitos, Calif.

Yang, X.Z., and Clausi, D.A. 2007. SAR sea ice image segmentation based on edge-preserving watersheds. In *Proceedings of the 4th Annual Canadian Conference on Computer and Robot Vision (CVR 2007)*, 28–30 May 2007, Montréal, Que. IEEE Computer Society, Los Alamitos, Calif. pp. 426–431.

Yu, Q., and Clausi, D.A. 2005. SAR sea-ice image analysis based on iterative region growing using semantics. *IEEE Transactions on Geoscience and Remote Sensing*, Vol. 45, No. 12, pp. 3919–3931.

Yu, Q., and Clausi, D.A., 2008. IRGS: image segmentation using edge penalties and region growing. *IEEE Transactions on Pattern Analysis and Machine Intelligence*, Vol. 30, No. 12, pp. 2126–2139.